Appl. Math. Mech. -Engl. Ed., **43**(10), 1531–1542 (2022)

APPLIED MATHEMATICS AND MECHANICS (ENGLISH EDITION)

https://doi.org/10.1007/s10483-022-2911-9

Enhancing suspension vibration reduction by diagonal inerter*

Meng YANG[1], Xingjiu LUO[1], Xiaoqiang ZHANG[1], Hu DING[2], Liqun CHEN[2,†]

1. Naval Medical Center of PLA, Shanghai 200433, China;
2. School of Mechanics and Engineering Sciences, Shanghai University, Shanghai 200072, China

(Received Apr. 17, 2022 / Revised Aug. 9, 2022)

Abstract The diagonal inerter is integrated into a suspension vibration reduction system (SVRS). The dynamic model of the SVRS with diagonal inerter and damping is established. The dynamic model is of strong geometric nonlinearity. The retaining nonlinearity up to cubic terms is validated under impact excitation. The conditions omitting the static deformation are determined. The effects of the diagonal inerter on the vibration reduction performance of the SVRS are explored under impact and random excitations. The vibration reduction performance of the proposed SVRS with both diagonal inerter and damping is better than that of either the SVRS without them or the SVRS with the diagonal damping only.

Key words suspension vibration reduction system (SVRS), diagonal inerter, verification calculation, geometric nonlinearity

Chinese Library Classification O322
2010 Mathematics Subject Classification 70K40

1 Introduction

Product damage and function failure caused by improper packing often occur in existing logistics transportation systems, and main factors of the damage refer to vibration and impact in logistics transportation, such as high/low-frequency vibration of products during the transportation by highway, railway, sea and air, and drop impact in handling process. In order to inhibit the influence of vibration on the transported goods effectively, it is required to take reasonable vibration reduction measures to protect the transported goods, and the suspension vibration reduction system (SVRS) is widely used in numerous cushion packaging technologies. In the previous research[1], the SVRS has been improved by introducing diagonal damping. However, there is still room for improvement in the vibration reduction performance of the SVRS. The inerter can achieve greater inertance with a smaller mass and increase the vibration isolation frequency band of the vibration reduction system. It is reasonable to believe that the performance of the SVRS can be further improved by introducing the diagonal inerter.

The inerter was created in 2002[2]. A classic research direction of the inerter was to combine the inerter with springs and dampers in different arrangements to form different vibration

* Citation: YANG, M., LUO, X. J., ZHANG, X. Q., DING, H., and CHEN, L. Q. Enhancing suspension vibration reduction by diagonal inerter. *Applied Mathematics and Mechanics* (*English Edition*), **43**(10), 1531–1542 (2022) https://doi.org/10.1007/s10483-022-2911-9

† Corresponding author, E-mail: lqchen@shu.edu.cn

isolation units, and then to compare their dynamic characteristics to choose a better one[3–5]. The inerters in these studies were basically linear. Due to the fact that the advent of the inerter has greatly expanded the development space of mechanical systems, the inerter has become more and more attractive in recent years, especially the study of nonlinear characteristics of the inerter and the application of the inerter in vibration suppression of building structures[6–8]. Wagg[9] and Ma et al.[10] pointed out that the studies on the nonlinearity of the inerter and its engineering exploration were the current development focus.

The nonlinearity of the inerter can be caused by a variety of reasons, and the corresponding nonlinear studies are also distinguished. One of the current research hotspots for the nonlinearity of the inerter is to introduce the inerter into nonlinear systems and study their dynamic characteristics. The scope of these studies is very broad, such as the inerter-based dynamic vibration absorber/inerter enhanced nonlinear energy sink[11–17], the tuned mass damper inerter/tuned inerter damper[18–22], the inerter-based vibration isolator[23–24], and the inerter-based vehicle suspension[25]. In these studies, the main system was nonlinear, while the inerter was linear. Therefore, the acceleration in the differential equation of motion was still linear.

In order to deeply study the nonlinearity of the inerter itself, some studies arranged the inerter horizontally and added stiffness and damping in the vertical direction to form an inerter-based vibration isolator[26–27]. Due to the geometric nonlinearity of the inerter, the acceleration in the differential equation of motion was nonlinear, which greatly increased the difficulty of modeling and analysis. By adding a horizontal inerter to the quasi-zero stiffness vibration isolator, a vibration isolator with both the geometric nonlinear stiffness and the inerter was obtained[28]. Similarly, by adding the horizontal inerter to the nonlinear stiffness vibration isolator using the diamond-shaped structure, a vibration isolator with both the geometric nonlinear stiffness and the inerter was also obtained[29]. This type of vibration isolator could achieve some performance improvements compared with the original vibration isolator, such as reducing the force transfer peak and bending the frequency response curves towards the low-frequency range to broaden the effective vibration isolation frequency band. In addition to the above vibration isolators, there was the vibration isolator in which the inerter element was connected in series with a horizontal stiffness[30–31]. This series structure of inerter and stiffness could achieve similar effects as the parallel structure of them, that is, it could suppress the bending trend of the transmissibility curve to the right.

Based on the above studies, it can be found that the nonlinear inerter is very beneficial for improving the vibration isolation performance, but the current studies on the nonlinearity of the inerter are not very sufficient[9]. Most of the studies on the nonlinearity of the inerter are to add the linear inerter to the nonlinear system. The main system is nonlinear, and the inerter itself is still linear and does not have geometric nonlinearity. A small number of studies on the nonlinear inerter were mainly based on the horizontal layout, and the studies on the diagonal inerter were rare. The diagonal inerter is just suitable for the SVRS. Therefore, the diagonal inerter can be introduced into the SVRS. In this way, the diagonal inerter can be used to enhance the performance of the SVRS, and the dynamic model of the diagonal inerter can also be studied in depth.

When establishing the differential equation of motion of the vibration reduction system with a diagonal inerter, simplifications are unavoidable. However, the simplifications need to deal with the relationship with accuracy so as not to cause large errors. The higher-order nonlinear terms were generally omitted in modeling. For this approximation, only a few studies[26,29] verified it, and most studies[28,32–34] did not verify it. The studies verifying it showed that omitting higher-order nonlinear terms would not cause large errors, especially if the Taylor series expansion was adopted. For static deformation, almost all studies did not consider the weight in modeling. However, a previous study[35] showed that when calculating the natural frequency and amplitude-frequency response of a structure with a nonlinear energy sink, whether or not the weight was taken into account could lead to different results. If the static deformation caused

by the weight was retained in the differential equation of motion, it would make it difficult to solve, especially when the analytical method was used. Therefore, the static deformation should be simplified during modeling. However, how to simplify the static deformation depends on the detailed verification calculation, and it cannot be omitted directly.

Based on the above discussion, an SVRS with diagonal inerter and damping is designed. Then, the dynamic model of this novel SVRS is established, and the influence of the static deformation of vibration reduction system on the dynamic response is emphatically studied. Finally, the novel SVRS is compared with the previous SVRS, and the similarity and difference between different SVRSs are discussed.

2 Dynamic model of SVRS with diagonal inerter and damping

Figure 1 shows the theoretical model of the SVRS with diagonal inerter and damping. There are, respectively, four springs, dampers, and inerters on the top and at the bottom of the SVRS to support the vibrated object diagonally, which have the same stiffness coefficient, damping coefficient, inertance coefficient, and original length. The position shown in Fig. 1 is the one where deformation has not occurred. The original length of the springs, dampers, and inerters is $HF = GE = AB = DC = l_0$, and the included angle with the horizontal direction is $\angle GHF = \angle HGE = \angle DAB = \angle ADC = \varphi_0$. The diagonal stiffness coefficient is K, the diagonal damping coefficient is C_1, and the diagonal inertance coefficient is b. Meanwhile, it is considered that the vertical damping coefficient is C_0, and the mass of the isolated object is M. When the system reaches equilibrium under the action of gravity, the gravity center of the isolated objects moves down by x_0, and then $\angle DAB = \angle ADC = \varphi_1$, and $\angle GHF = \angle HGE = \varphi_2$. The lengths of springs, dampers, and inerters become $AB = CD = l_1$ and $HF = GE = l_2$ with the equations as follows:

$$l_1 = \sqrt{l_0^2 \cos^2 \varphi_0 + (l_0 \sin \varphi_0 - x_0)^2},$$
$$l_2 = \sqrt{l_0^2 \cos^2 \varphi_0 + (l_0 \sin \varphi_0 + x_0)^2}.$$

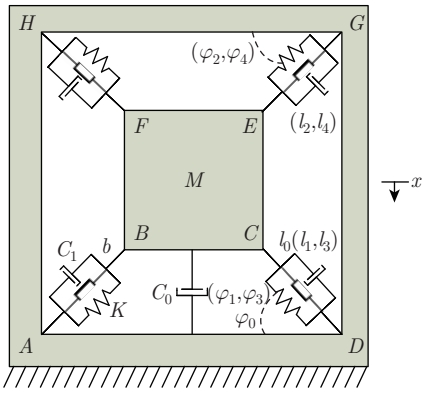

Fig. 1 The SVRS with diagonal inerter and damping (color online)

In the static state, the equilibrium equation of the isolated object is as follows:

$$\begin{cases} 4K(l_0 - l_1)\sin\varphi_1 + 4K(l_2 - l_0)\sin\varphi_2 = Mg, \\ \sin\varphi_1 = (l_0 \sin\varphi_0 - x_0)/l_1, \\ \sin\varphi_2 = (l_0 \sin\varphi_0 + x_0)/l_2. \end{cases} \tag{1}$$

Choose the static equilibrium position as the coordinate origin. Then, a rectangular coordinate system is established. Taking downward as the positive direction, the displacement of the isolated object is x. Then, the lengths of springs, dampers, and inerters are $AB = CD = l_3$ and $HF = GE = l_4$ with the equations as follows:

$$l_3 = \sqrt{l_1^2 \cos^2 \varphi_1 + (l_1 \sin \varphi_1 - x)^2}, \tag{2}$$

$$l_4 = \sqrt{l_2^2 \cos^2 \varphi_2 + (l_2 \sin \varphi_2 + x)^2}. \tag{3}$$

The vertical dynamic equation of the system is

$$\begin{aligned} M\ddot{x} = {} & Mg - C_0\dot{x} - 4b(\ddot{l}_0 - \ddot{l}_3)\sin\varphi_3 - 4b(\ddot{l}_4 - \ddot{l}_0)\sin\varphi_4 - 4C_1(\dot{l}_0 - \dot{l}_3)\sin\varphi_3 \\ & - 4C_1(\dot{l}_4 - \dot{l}_0)\sin\varphi_4 - 4K(l_0 - l_3)\sin\varphi_3 - 4K(l_4 - l_0)\sin\varphi_4, \end{aligned}$$

where $\sin\varphi_3 = (l_1 \sin\varphi_1 - x)/l_3$, and $\sin\varphi_4 = (l_2 \sin\varphi_2 + x)/l_4$. Since $\dot{l}_0 = 0$ and $\ddot{l}_0 = 0$, the above equation can be converted to

$$\begin{aligned} M\ddot{x} = {} & Mg - C_0\dot{x} + 4b\ddot{l}_3 \sin\varphi_3 - 4b\ddot{l}_4 \sin\varphi_4 + 4C_1\dot{l}_3 \sin\varphi_3 - 4C_1\dot{l}_4 \sin\varphi_4 \\ & - 4K(l_0 - l_3)\sin\varphi_3 - 4K(l_4 - l_0)\sin\varphi_4. \end{aligned} \tag{4}$$

The above equation is the vertical dynamic equation of the SVRS with diagonal inerter and damping. It is deduced that

$$\dot{l}_3 = -\dot{x}\sin\varphi_3, \quad \dot{l}_4 = \dot{x}\sin\varphi_4, \quad \ddot{l}_3 = \frac{\dot{x}^2}{l_3}\cos^2\varphi_3 - \ddot{x}\sin\varphi_3, \quad \ddot{l}_4 = \frac{\dot{x}^2}{l_4}\cos^2\varphi_4 + \ddot{x}\sin\varphi_4.$$

$\sin\varphi_3$, $\sin\varphi_4$, $\dot{l}_3$, $\dot{l}_4$, $\ddot{l}_3$, and $\ddot{l}_4$ are substituted into Eq. (4), and it is noted that $\sin^2\varphi_3 = 1 - \cos^2\varphi_3 = 1 - (l_0/l_3)^2\cos^2\varphi_0$, and $\sin^2\varphi_4 = 1 - (l_0/l_4)^2\cos^2\varphi_0$. Then, Eq. (4) is finally transformed into

$$\begin{aligned} M\ddot{x} = {} & Mg - C_0\dot{x} + 4b\Big(\dot{x}^2\frac{l_0\sin\varphi_0 - x_0 - x}{l_0^2}\Big(\frac{l_0}{l_3}\Big)^4\cos^2\varphi_0 - \ddot{x}\Big(1 - \Big(\frac{l_0}{l_3}\Big)^2\cos^2\varphi_0\Big)\Big) \\ & - 4b\Big(\dot{x}^2\frac{l_0\sin\varphi_0 + x_0 + x}{l_0^2}\Big(\frac{l_0}{l_4}\Big)^4\cos^2\varphi_0 + \ddot{x}\Big(1 - \Big(\frac{l_0}{l_4}\Big)^2\cos^2\varphi_0\Big)\Big) \\ & - 4C_1\dot{x}(1 - (l_0/l_3)^2\cos^2\varphi_0) - 4C_1\dot{x}(1 - (l_0/l_4)^2\cos^2\varphi_0) \\ & - 4K(l_0/l_3 - 1)(l_0\sin\varphi_0 - x_0 - x) - 4K(1 - l_0/l_4)(l_0\sin\varphi_0 + x_0 + x). \end{aligned} \tag{5}$$

When the higher-order terms are omitted and the small quantity is not considered, l_0/l_3 and l_0/l_4 are expanded by the Taylor series. The results can be obtained as follows:

$$\begin{aligned} \frac{l_0}{l_3} = {} & \frac{1}{\sqrt{1 - \frac{2(x_0+x)l_0\sin\varphi_0 - (x_0+x)^2}{l_0^2}}} \\ = {} & 1 + \frac{x_0 + x}{l_0}\sin\varphi_0 - \frac{1}{2l_0^2}(x_0 + x)^2 + \frac{3}{2l_0^2}\sin^2\varphi_0(x_0 + x)^2 \\ & - \frac{3}{2l_0^3}\sin\varphi_0(x_0 + x)^3 + \frac{5}{2l_0^3}\sin^3\varphi_0(x_0 + x)^3, \\ \frac{l_0}{l_4} = {} & 1 - \frac{x_0 + x}{l_0}\sin\varphi_0 - \frac{1}{2l_0^2}(x_0 + x)^2 + \frac{3}{2l_0^2}\sin^2\varphi_0(x_0 + x)^2 \\ & + \frac{3}{2l_0^3}\sin\varphi_0(x_0 + x)^3 - \frac{5}{2l_0^3}\sin^3\varphi_0(x_0 + x)^3. \end{aligned}$$

Substituting the computed results above into the right half part of Eq. (5) and omitting the higher-order terms yield

$$\begin{aligned}M\ddot{x} = {} & Mg - C_0\dot{x} + 4b\Big(\Big(\frac{64\cos^2\varphi_0\sin^4\varphi_0}{l_0^4} - \frac{48\cos^2\varphi_0\sin^2\varphi_0}{l_0^4} + \frac{4\cos^2\varphi_0}{l_0^4}\Big)(x_0+x)^3 \\ & + \Big(\frac{8\cos^2\varphi_0\sin^2\varphi_0}{l_0^2} - \frac{2\cos^2\varphi_0}{l_0^2}\Big)(x_0+x)\Big)\dot{x}^2 \\ & - 8b\Big(\sin^2\varphi_0 + \frac{1}{l_0^2}(\cos^2\varphi_0 - 4\cos^2\varphi_0\sin^2\varphi_0)(x_0+x)^2\Big)\ddot{x} \\ & - 8C_1\Big(\sin^2\varphi_0 + \frac{1}{l_0^2}(\cos^2\varphi_0 - 4\cos^2\varphi_0\sin^2\varphi_0)(x_0+x)^2\Big)\dot{x} \\ & - 8K\Big(\sin^2\varphi_0(x_0+x) + \frac{1}{2l_0^2}(1 - 6\sin^2\varphi_0 + 5\sin^4\varphi_0)(x_0+x)^3\Big). \end{aligned} \tag{6}$$

It can be seen from Eq. (1) that

$$Mg = 4K\Big(\frac{l_0}{l_1} - 1\Big)(l_0\sin\varphi_0 - x_0) + 4K\Big(1 - \frac{l_0}{l_2}\Big)(l_0\sin\varphi_0 + x_0). \tag{7}$$

Conduct the Taylor series expansion of l_0/l_1 and l_0/l_2 in reference to the expansion method of l_0/l_3 and l_0/l_4, and substitute the results obtained into the right half part of Eq. (7). Then, we can obtain

$$Mg = 8K\Big(\sin^2\varphi_0 x_0 + \frac{1}{2l_0^2}(1 - 6\sin^2\varphi_0 + 5\sin^4\varphi_0)x_0^3\Big). \tag{8}$$

In order to simplify the differential equation of motion, Eq. (8) is brought into Eq. (6), and it is assumed that x_0 is a small quantity and then omitted. We can obtain

$$\begin{aligned} & M\ddot{x} + C_0\dot{x} - 8b\Big(\frac{e_0}{l_0^4}x^3 + \frac{f_0}{l_0^2}x\Big)\dot{x}^2 + 8b\Big(a_0 + \frac{d_0}{l_0^2}x^2\Big)\ddot{x} \\ & + 8C_1\Big(a_0 + \frac{d_0}{l_0^2}x^2\Big)\dot{x} + 8K\Big(a_0 x + \frac{b_0}{l_0^2}x^3\Big) = 0, \end{aligned} \tag{9}$$

where $a_0 = \sin^2\varphi_0$, $b_0 = (1 - 6\sin^2\varphi_0 + 5\sin^4\varphi_0)/2$, $d_0 = \cos^2\varphi_0 - 4\cos^2\varphi_0\sin^2\varphi_0$, $e_0 = 32\cos^2\varphi_0\sin^4\varphi_0 - 24\cos^2\varphi_0\sin^2\varphi_0 + 2\cos^2\varphi_0$, and $f_0 = 4\cos^2\varphi_0\sin^2\varphi_0 - \cos^2\varphi_0$.

The above is the derivation process of the dynamic model of the SVRS with diagonal inerter and damping. From the above process, it can be seen that the geometric nonlinear force of diagonal inerter is not only related to the acceleration, but also the square term of velocity and the square and cubic terms of displacement, showing a high degree of geometric nonlinearity, which is much more complex than the geometric nonlinear forces of diagonal stiffness and diagonal damping.

3 Accuracy verification of dynamic model

The simplification in the derivation process of Section 2 mainly appears in two parts. The first part is the expansions of l_0/l_3, l_0/l_4, l_0/l_1, and l_0/l_2, which are carried out by the Taylor series, and the accuracy of the Taylor series expansion has been verified by other researchers[26,29]. In this paper, the parameters are set as $M = 50\,\mathrm{kg}$, $b = 10\,\mathrm{kg}$, $C_0 = 300\,\mathrm{N\cdot s/m}$, $C_1 = 600\,\mathrm{N\cdot s/m}$, $K = 50\,000\,\mathrm{N/m}$, $l_0 = 0.1\,\mathrm{m}$, $\varphi_0 = \pi/7$, and $-0.05\,\mathrm{m} \leqslant x \leqslant 0.05\,\mathrm{m}$. The comparison between the exact expression and the approximate expression (the Taylor series expansion) of l_0/l_3 and l_0/l_4 is shown in Fig. 2.

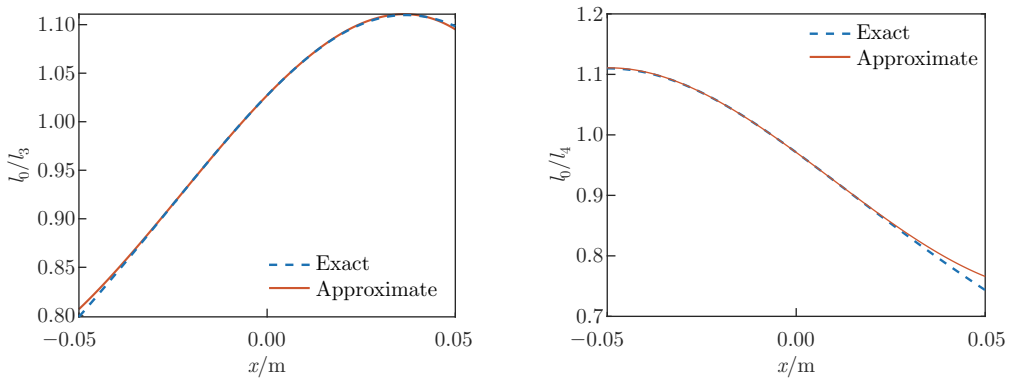

Fig. 2 Comparison between the exact expression and the approximate expression of l_0/l_3 and l_0/l_4 (color online)

It can be seen from Fig. 2 that within the variation range of the displacement, the approximate expressions of l_0/l_3 and l_0/l_4 have high precision and meet the use requirements. The second part of simplification of the derivation process mainly occurs in assuming that x_0 is a small quantity and omitted, which is verified below. Retaining x_0, Eq. (9) can be transformed into the following form:

$$M\ddot{x} + C_0\dot{x} - 8b\Big(\frac{e_0}{l_0^4}(x_0+x)^3 + \frac{f_0}{l_0^2}(x_0+x)\Big)\dot{x}^2 + 8b\Big(a_0 + \frac{d_0}{l_0^2}(x_0+x)^2\Big)\ddot{x}$$
$$+ 8C_1\Big(a_0 + \frac{d_0}{l_0^2}(x_0+x)^2\Big)\dot{x} + 8K\Big(a_0x + \frac{b_0}{l_0^2}(3x_0^2x + 3x_0x^2 + x^3)\Big) = 0. \tag{10}$$

Under the impact excitation, the fitting degree of the output responses of the dynamic model omitting x_0 and the dynamic model retaining x_0 is verified. Considering the base motion, the vibration displacement of the outer frame $ADGH$ is q, and $y = x - q$. Then, Eqs. (9) and (10) can be transformed into

$$(M + 8ba_0)\ddot{y} + (C_0 + 8C_1a_0)\dot{y} + 8Ka_0y - 8b\Big(\frac{e_0}{l_0^4}y^3 + \frac{f_0}{l_0^2}y\Big)\dot{y}^2$$
$$+ \frac{8bd_0y^2\ddot{y}}{l_0^2} + \frac{8C_1d_0y^2\dot{y}}{l_0^2} + \frac{8Kb_0y^3}{l_0^2} = -M\ddot{q}, \tag{11}$$

$$\Big(M + 8ba_0 + 8b\frac{d_0}{l_0^2}x_0^2\Big)\ddot{y} + \Big(C_0 + 8C_1a_0 + 8C_1\frac{d_0}{l_0^2}x_0^2\Big)\dot{y} + 8\Big(Ka_0 + 3K\frac{b_0}{l_0^2}x_0^2\Big)y$$
$$- 8b\Big(\frac{e_0}{l_0^4}(x_0+y)^3 + \frac{f_0}{l_0^2}(x_0+y)\Big)\dot{y}^2 + \frac{8bd_0(2x_0y+y^2)\ddot{y}}{l_0^2} + \frac{8C_1d_0(2x_0y+y^2)\dot{y}}{l_0^2}$$
$$+ \frac{8Kb_0(3x_0y+y^3)}{l_0^2} = -M\ddot{q}. \tag{12}$$

The half-sine wave of acceleration is used to represent the impact excitation, which is as follows:

$$\ddot{q} = \begin{cases} 10\sin\Big(\dfrac{\pi}{0.01}t\Big), & 0\,\mathrm{s} \leqslant t \leqslant 0.01\,\mathrm{s}, \\ 0, & 0.01\,\mathrm{s} < t. \end{cases} \tag{13}$$

In order to observe the effects of the suspension angle φ_0 and the stiffness K (which affects x_0) on the fitting degree of the output responses of the dynamic model omitting x_0 and the

dynamic model retaining x_0, the system parameters are set as follows: $M = 50\,\mathrm{kg}$, $b = 10\,\mathrm{kg}$, $C_0 = 300\,\mathrm{N\cdot s/m}$, $C_1 = 600\,\mathrm{N\cdot s/m}$, $40\,000\,\mathrm{N/m} \leqslant K \leqslant 60\,000\,\mathrm{N/m}$, $l_0 = 0.1\,\mathrm{m}$, and $0.2 \leqslant \varphi_0 \leqslant 1.09$. The minimum error between the dynamic model omitting x_0 and the dynamic model retaining x_0 is calculated by the ergodic optimization method[1]. The Runge-Kutta method is used to solve the differential equation of motion of the SVRS in this paper. The error e is set as follows:

$$e = \sqrt{\sum_{i=1}^{N} \ddot{y}_i^2}, \quad \ddot{y} = \ddot{y}_g - \ddot{y}_r, \tag{14}$$

where $\ddot{y}_g$ and $\ddot{y}_r$ represent the accelerations of Eqs. (11) and (12), respectively, and N represents the number of sampling points. The calculation accuracy depends on the sampling step sizes of the stiffness K and the suspension angle φ_0. Therefore, three different combinations of the step size are given. After calculation, the errors are shown in Fig. 3.

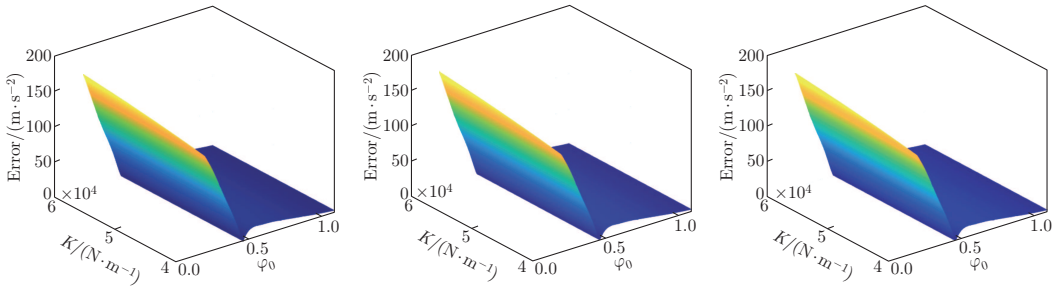

(a) Step sizes of K and φ_0 are 500 N/m and 0.005

(b) Step sizes of K and φ_0 are 200 N/m and 0.002

(c) Step sizes of K and φ_0 are 100 N/m and 0.001

Fig. 3 Errors between omitting x_0 versus retaining x_0 (color online)

It can be seen from Fig. 3 that different combinations of the stiffness K and the suspension angle φ_0 can cause a dramatic change in the error, which means that the static deformation x_0 has an important effect on the output response of the SVRS with diagonal inerter and damping. This indicates that the verification should be performed before omitting the static deformation, and it can be omitted only when the parameters are appropriate. It also can be seen from Fig. 3 that the effect of the suspension angle φ_0 on the error is obviously greater than that of the stiffness K.

The stiffness K and the suspension angle φ_0 are (60 000 N/m, 0.465 0), (60 000 N/m, 0.464 0), and (60 000 N/m, 0.464 0) in Figs. 3(a), 3(b), and 3(c), respectively, when the error is the minimum. The parameters are the same in Figs. 3(b) and 3(c), which means that improving the calculation accuracy can no longer change the optimization result. Therefore, it can be concluded that if the stiffness K and the suspension angle φ_0 are set as 60 000 N/m and 0.464 0, the error is the minimum. When $K = 60\,000\,\mathrm{N/m}$ and $\varphi_0 = 0.464\,0$, the comparison among the dynamic model omitting x_0 (Eq. (11)), the dynamic model retaining x_0 (Eq. (12)), and the original dynamic model (Eq. (5)) is shown in Fig. 4.

Based on the above analysis, the response of the dynamic model of the SVRS omitting x_0 can be well fitted with the responses of that retaining x_0 and the original dynamic model, when $K = 60\,000\,\mathrm{N/m}$ and $\varphi_0 = 0.464\,0$. Therefore, $K = 60\,000\,\mathrm{N/m}$ and $\varphi_0 = 0.464\,0$ in the subsequent analysis, and other parameters remain unchanged unless otherwise specified, that is, $M = 50\,\mathrm{kg}$, $b = 10\,\mathrm{kg}$, $C_0 = 300\,\mathrm{N\cdot s/m}$, $C_1 = 600\,\mathrm{N\cdot s/m}$, and $l_0 = 0.1\,\mathrm{m}$.

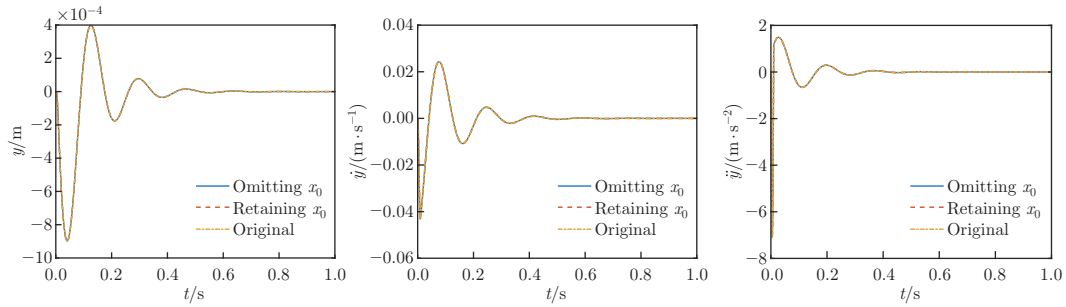

Fig. 4 Comparison among the dynamic model omitting x_0, the dynamic model retaining x_0, and the original dynamic model (color online)

4 Influence of inerter on SVRS with diagonal inerter and damping

Change the inerter b to observe the dynamic responses of the SVRS with diagonal inerter and damping under impact and random excitations. The differential equation of motion is shown as Eq. (11). The impact excitation is the same as that in Section 3. The random excitation adopts the off-road vibration data of the rear chassis of a tracked ambulance, with a duration of 176.124 s and a sampling frequency of 250 Hz. The time-domain waveform is shown in Fig. 5.

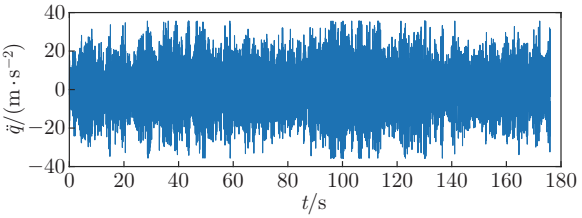

Fig. 5 Random excitation (color online)

The above excitation is brought into the differential equation of motion for calculation. Under impact excitation, the inerter b is changed as follows: 10 kg, 20 kg, 30 kg, 40 kg, 50 kg, and under random exciation, the inerter b is changed as follows: 10 kg, 20 kg, 30 kg, 40 kg, 50 kg, 150 kg, 300 kg, 500 kg. The other parameters are the same as those in Section 3. The dynamic responses under impact and random excitations are shown in Fig. 6.

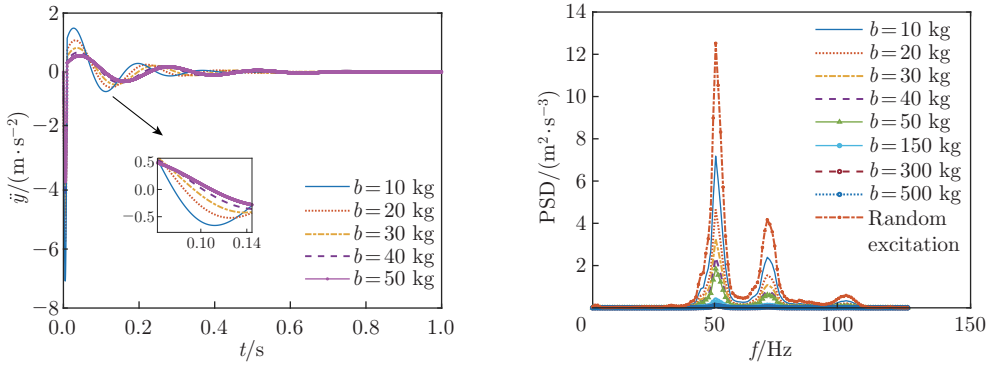

(a) Response under impact excitation (b) Response under random excitation

Fig. 6 Dynamic responses, where PSD means the power spectral density (color online)

As can be seen from Fig. 6, with the increase in the inerter b, both the peak values of the acceleration under impact excitation and the PSD under random excitation are getting smaller and smaller, which shows that a larger inerter b is beneficial to the SVRS and can obviously improve the vibration reduction efficiency. However, it does not show the trend that the SVRS becomes a rigid body with the increase in the inerter. This may indicate that the ideal model of the inerter may not have the characteristic that a big enough inerter can cause the system to become a rigid body.

5 Comparative study of different types of SVRS

Under impact and random excitations, the vibration reduction performances of three types of SVRSs, i.e., Type I: a general SVRS (an SVRS without diagonal inerter and damping), Type II: an SVRS with the diagonal damping only, and Type III: an SVRS with diagonal inerter and damping, are compared. According to Ref. [1], the differential equations of motion of Types I and II are as follows:

$$M\ddot{x} + C_0\dot{x} + 8K\left(a_0 x + \frac{b_0}{l_0^2}x^3\right) = 0, \tag{15}$$

$$M\ddot{x} + C_0\dot{x} + 8C_1\left(a_0 + \frac{d_0}{l_0^2}x^2\right)\dot{x} + 8K\left(a_0 x + \frac{b_0}{l_0^2}x^3\right) = 0. \tag{16}$$

The meanings of relevant parameters in Eqs. (15) and (16) are the same as those in Eq. (9). Let $y = x - q$. Then, Eqs. (15) and (16) can be transformed into the following forms:

$$M\ddot{y} + C_0\dot{y} + 8Ka_0 y + \frac{8Kb_0y^3}{l_0^2} = -M\ddot{q}, \tag{17}$$

$$M\ddot{y} + (C_0 + 8C_1a_0)\dot{y} + 8Ka_0 y + \frac{8C_1d_0y^2\dot{y}}{l_0^2} + \frac{8Kb_0y^3}{l_0^2} = -M\ddot{q}. \tag{18}$$

The impact excitation and the parameters are the same as those in Section 3, and the random excitation is the same as that in Section 4. Under impact and random excitations, the comparison among three SVRSs can be obtained, such as those shown in Fig. 7.

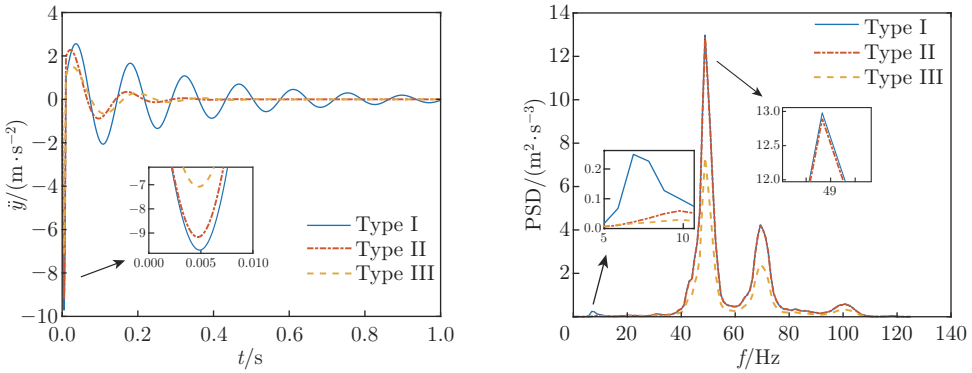

(a) Impact excitation (b) Random excitation

Fig. 7 Comparison among three SVRSs (color online)

It can be seen from Fig. 7 that the vibration reduction performance of the SVRS with diagonal inerter and damping is the highest under both impact and random excitations, which shows that the diagonal inerter can obviously improve the vibration reduction performance of

the SVRS. Under impact excitation, the anti-impact performance of the SVRS with diagonal inerter and damping is slightly better than that of the SVRS with diagonal damping only (obviously better at the first peak and the second peak), but obviously better than that of the general SVRS. Under random excitation, the SVRS with diagonal inerter and damping is obviously superior to the SVRS with diagonal damping only and the general SVRS. From the partial view of Fig. 7(b), it can be seen that under random excitation, the PSD of the SVRS with diagonal damping only is basically the same as that of the general SVRS at a high frequency, but the former is obviously better than the latter at a low frequency, which shows that the introduction of diagonal damping is still beneficial to the attenuation of random excitation.

6 Conclusions

An SVRS is proposed by introducing diagonal inerter and damping. Its differential equation of motion is established and simplified with the verification. For different sets of parameters, the dynamic responses are respectively evaluated under impact and random excitations. Finally, the dynamic responses of different SVRSs are compared under impact and random excitations. Therefore, in this study, the following conclusions can be drawn based on these investigations.

(i) The introduction of diagonal inerter leads to strongly nonlinear differential equation of motion, while the dynamics can be captured by retaining the square and the cubic terms. The geometric nonlinear force of diagonal inerter is a function with respect to not only the acceleration but also the square term of the velocity and the square and the cubic terms of the displacement.

(ii) The response of the SVRS depends generally on its static deformation. The static deformation can be omitted only for appropriate parameters.

(iii) The diagonal inerter can significantly improve the vibration reduction performance of the SVRS under both impact and random excitations, especially the random excitation. The larger the inerter is, the better the performance is. Notably, while increasing the inerter, the engineering practice should be considered to avoid the system being a rigid body due to excessive inerter.

References

[1] YANG, M., ZHANG, J., and LUO, X. J. Research on new types of suspension vibration reduction systems (SVRSs) with geometric nonlinear damping. *Mathematical Problems in Engineering*, **2021**, 6627693 (2021)

[2] SMITH, M. C. Synthesis of mechanical networks: the inerter. *IEEE Transactions on Automatic Control*, **47**(10), 1648–1662 (2002)

[3] HU, Y. L., CHEN, M. Z. Q., SHU, Z., and HUANG, L. X. Analysis and optimisation for inerter-based isolators via fixed-point theory and algebraic solution. *Journal of Sound and Vibration*, **346**, 17–36 (2015)

[4] CAO, F., CHEN, M. Z. Q., and HU, Y. L. Seismic isolation performance evaluation for a class of inerter-based low-complexity isolators. *Shock and Vibration*, **2020**, 8837822 (2020)

[5] HU, Y. L. and CHEN, M. Z. Q. Low-complexity passive vehicle suspension design based on element-number-restricted networks and low-order admittance networks. *Journal of Dynamic Systems Measurement and Control-Transactions of the ASME*, **140**(10), 101014 (2018)

[6] SHEN, W. A., LONG, Z. T., CAI, L., NIYITANGAMAHORO, A., ZHU, H. P., LI, Y. M., and QIU, C. X. An inerter-based electromagnetic damper for civil structures: modeling, testing, and seismic performance. *Mechanical Systems and Signal Processing*, **173**, 109070 (2022)

[7] WANG, H., SHEN, W. A., LI, Y. M., ZHU, H. P., and ZHU, S. Y. Dynamic behavior and seismic performance of base-isolated structures with electromagnetic inertial mass dampers: analytical solutions and simulations. *Engineering Structures*, **246**, 113072 (2021)

[8] SHEN, W. A., NIYITANGAMAHORO, A., FENG, Z. Q., and ZHU, H. P. Tuned inerter dampers for civil structures subjected to earthquake ground motions: optimum design and seismic performance. *Engineering Structures*, **198**, 109470 (2019)

[9] WAGG, D. J. A review of the mechanical inerter: historical context, physical realisations and nonlinear applications. *Nonlinear Dynamics*, **104**(1), 13–34 (2021)

[10] MA, R. S., BI, K. M., and HAO, H. Inerter-based structural vibration control: a state-of-the-art review. *Engineering Structures*, **243**, 112655 (2021)

[11] XU, Q., LUO, Y. Q., YAO, H. L., ZHAO, L. C., and WEN, B. C. Eliminating the fluid-induced vibration and improving the stability of the rotor/seal system using the inerter-based dynamic vibration absorber. *Shock and Vibration*, **2019**, 1746563 (2019)

[12] CHANG, W. W., JIN, X. L., HUANG, Z. L., and CAI, G. Q. Random response of nonlinear system with inerter-based dynamic vibration absorber. *Journal of Vibration Engineering & Technol*ogies, **9**(8), 1903–1909 (2021)

[13] QIAN, F. and ZUO, L. Tuned nonlinear spring-inerter-damper vibration absorber for beam vibration reduction based on the exact nonlinear dynamics model. *Journal of Sound and Vibration*, **509**, 116246 (2021)

[14] ZHANG, Y. W., LU, Y. N., ZHANG, W., TENG, Y. Y., YANG, H. X., YANG, T. Z., and CHEN, L. Q. Nonlinear energy sink with inerter. *Mechanical Systems and Signal Processing*, **125**, 52–64 (2019)

[15] DUAN, N., WU, Y. H., SUN, X. M., and ZHONG, C. Q. Vibration control of conveying fluid pipe based on inerter enhanced nonlinear energy sink. *IEEE Transactions on Circuits and Systems — I : Regular Papers*, **68**(4), 1610–1623 (2021)

[16] JAVIDIALESAADI, A. and WIERSCHEM, N. E. An inerter-enhanced nonlinear energy sink. *Mechanical Systems and Signal Processing*, **129**, 449–454 (2019)

[17] ZENG, Y. C., DING, H., DU, R. H., and CHEN, L. Q. A suspension system with quasi-zero stiffness characteristics and inerter nonlinear energy sink. *Journal of Vibration and Control*, **28**(1-2), 143–158 (2020)

[18] KAKOU, P. and BARRY, O. Simultaneous vibration reduction and energy harvesting of a nonlinear oscillator using a nonlinear electromagnetic vibration absorber-inerter. *Mechanical Systems and Signal Processing*, **156**, 107607 (2021)

[19] GUO, C. A. and LUO, A. C. J. Symmetric and asymmetric periodic motions of a nonlinear oscillator with a tuned mass damper inerter. *The European Physical Journal Special Topics*, **230**(18-20), 3533–3549 (2021)

[20] DE DOMENICO, D. and RICCIARDI, G. Optimal design and seismic performance of tuned mass damper inerter (TMDI) for structures with nonlinear base isolation systems. *Earthquake Engineering & Structural Dynamics*, **47**(12), 2539–2560 (2018)

[21] RADU, A., LAZAR, I. F., and NEILD, S. A. Performance-based seismic design of tuned inerter dampers. *Structural Control & Health Monitoring*, **26**(5), e2346 (2019)

[22] ZHANG, R. F., WU, M. J., REN, X. S., and PAN, C. Seismic response reduction of elastoplastic structures with inerter systems. *Engineering Structures*, **230**, 111661 (2021)

[23] WANG, Y., LI H. X., CHENG, C., DING, H., and CHEN, L. Q. Dynamic performance analysis of a mixed-connected inerter-based quasi-zero stiffness vibration isolator. *Structural Control & Health Monitoring*, **27**(10), e2604 (2020)

[24] WANG, Y., LI, H. X., JIANG, W. A., DING, H., and CHEN, L. Q. A base excited mixed-connected inerter-based quasi-zero stiffness vibration isolator with mistuned load. *Mechanics of Advanced Materials and Structures* (2021) https://doi.org/10.1080/15376494.2021.1922961

[25] LIU, X. F., JIANG, J. Z., HARRISON, A., and NA, X. X. Truck suspension incorporating inerters to minimise road damage. *Proceedings of the Institution of Mechanical Engineers Part D-Journal of Automobile Engineering*, **234**(10-11), 2693–2705 (2020)

[26] WANG, Y., WANG, R. C., MENG, H. D., and ZHANG, B. Y. An investigation of the dynamic performance of lateral inerter-based vibration isolator with geometrical nonlinearity. *Archive of Applied Mechanics*, **89**(9), 1953–1972 (2019)

[27] MORAES, F. D., SILVEIRA, M., and GONCALVES, P. J. P. On the dynamics of a vibration isolator with geometrically nonlinear inerter. *Nonlinear Dynamics*, **93**(3), 1325–1340 (2018)

[28] YANG, J., JIANG, J. Z., and NEILD, S. A. Dynamic analysis and performance evaluation of nonlinear inerter-based vibration isolators. *Nonlinear Dynamics*, **99**(3), 1823–1839 (2019)

[29] WANG, Y., LI, H. X., CHENG, C., DING, H., and CHEN, L. Q. A nonlinear stiffness and nonlinear inertial vibration isolator. *Journal of Vibration and Control*, **27**(11-12), 1336–1352 (2020)

[30] LIU, C. R., YU, K. P., LIAO, B. P., and HU, R. P. Enhanced vibration isolation performance of quasi-zero-stiffness isolator by introducing tunable nonlinear inerter. *Communications in Nonlinear Science and Numerical Simulation*, **95**, 105654 (2021)

[31] LIAO, X., ZHANG, N., DU, X. F., and ZHANG, W. J. Theoretical modeling and vibration isolation performance analysis of a seat suspension system based on a negative stiffness structure. *Applied Sciences-Basel*, **11**(15), 6928 (2021)

[32] ZHANG, J. N., YANG, S. P., LI, S. H., LU, Y. J., and DING, H. Influence of vehicle-road coupled vibration on tire adhesion based on nonlinear foundation. *Applied Mathematics and Mechanics* (*English Edition*), **42**(5), 607–624 (2021) https://doi.org/10.1007/s10483-021-2724-6

[33] LU, Z. Q., LI, K., DING, H., and CHEN, L. Q. Nonlinear energy harvesting based on a modified snap-through mechanism. *Applied Mathematics and Mechanics* (*English Edition*), **40**(1), 167–180 (2019) https://doi.org/10.1007/s10483-019-2408-9

[34] WANG, D., HAO, Z. F., CHEN, F. Q., and CHEN, Y. S. Nonlinear energy harvesting with dual resonant zones based on rotating system. *Applied Mathematics and Mechanics* (*English Edition*), **42**(2), 275–290 (2021) https://doi.org/10.1007/s10483-021-2698-8

[35] CHEN, L. Q., LI, X., LU, Z. Q., ZHANG, Y. W., and DING, H. Dynamic effects of weights on vibration reduction by a nonlinear energy sink moving vertically. *Journal of Sound and Vibration*, **451**, 99–119 (2019)